www.cafetinnova.org

Indexed in
Scopus Compendex and Geobase Elsevier,
Geo-Ref Information Services-USA, List B of Scientific
Journals, Poland, Directory of Research Journals

ISSN 0974-5904, Volume 09, No. 02

International Journal of Earth Sciences and Engineering

April 2016, P.P.521-527

Dynamic Simulation Analysis of Slab Ballastless Track Subgrade of High-Speed Railway

ZUYIN ZOU[1,2*], XIANGHUI KONG[3], HANG CHEN[1,2] AND XUEMEI LONG[1]
[1]*School of Civil Engineering, Sichuan Agricultural University, Dujiangyan 611830, China*
[2]*School of Civil Engineering, Southwest Jiaotong University, Chengdu 610031, China*
[3]*School of Transportation Engineering, Shandong Jianzhu University, Jinan 250101, China*
Email: *chenh0727@126.com*

Abstract: With the development of high speed railway, ballastless track has been more widely used because of its own merits. Different track types lead to changes of dynamic properties in the railway structure. To discuss the dynamic interaction in the system of track and subgrade under train loads, the dynamic simulation method of ballastless track-subgrade system was studied using the ABAQUS finite element software. Based on this, the 3D model of slab ballastless track-subgrade in SuiYu railway was established. Through analysis of simulation results, the distribution law of dynamic stress of slab track and subgrade was acquired, and the effect of train speed on the dynamic property of track and soil subgrade was investigated. The research results indicate that along railway cross section, the dynamic stress of track structure is distributed unevenly, while it is more uniform on the surface of subgrade. Meanwhile, the dynamic stress of track and subgrade surface substantially increases linearly with train speed, but the attenuation law of dynamic stress along subgrade depth has little effect by the speed.

Keywords: *ballastless track, high-speed railway, dynamic properties, numerical simulation, train speed*

1. Introduction

To improve the stability and regularity of tracks during trains' high-speed running, systematic research on replacing granular railway ballast with overall solidified track bed constituted by materials like concrete, asphalt mixture and so forth, namely the research on ballastless track structure, has been carried out successively in various countries of the world since the early 1960s, which has been adopted as the main technological policy of developing high-speed railway [1]. Practice indicates that compared with traditional ballast track, ballastless track owns several merits listed as below: high stability, long-time retainability of track geometrical shape, obviously reduced maintenance workload and no splashing of ballast. With the progress of high-speed railway of heavy load, train-track dynamic interaction is intensified drastically [2].

The foundations of tracks - subgrades, especially those soil-made roadbeds, are not only the major bearers of trains' dynamic loads but the relatively weaker part in the whole tracks' structure due to subgrades being consisted of granular materials, both of which determine the dynamic characteristics of subgrades and become the key affecting the stability as well as safety concerning railways' whole system [3][4]. Therefore, it is necessary to master the stress-bearing condition and change law of subgrade structure in time so that bases for track maintenance plan of high-speed railways can be offered, which guarantees railway track's good and balanced condition[5]-[8].

In this paper, with the structure of Suining-Chongqing railway track as the prototype, a study on simulating calculation method of track (ballastless)-subgrade system power is conducted by adopting finite-element software ABAQUS and based on this, the influences of trains' running speed on track structure and soil-made subgrade's dynamic properties are discussed, which can be used as a reference when it comes to the design of ballastless track subgrade and selection of mechanical parameters.

2. Simulation Model of Track (Ballastless)-Subgrade System

2.1 Model Structure

Figure 1 is the dynamics model of track (ballastless)-subgrade system. Things of the model from top to bottom are respectively steel rail, track slab, CA mortar, concrete base, surface layer of roadbed, bottom layer of roadbed, subgrade body and foundation, which are all simulated as the 8-node entity element; contact among interfaces are achieved with TIE to keep the coordination of deformation between various layers; elastic pads and fasteners between steel rails and track slabs are simulated with spring-damping element.

Steel rails, track slabs, CA mortar and concrete base are deemed as isotropic elastic materials; surface layer of roadbed, bottom layer of roadbed, roadbed body

and foundation are regarded as the Drucker Prager's elastoplastic materials [9].

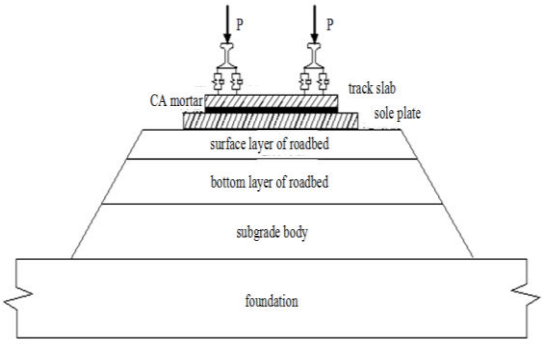

Figure 1: *Dynamic model of ballastless track-subgrade system*

2.2 Train Load

In reference [10], train loads are simulated with a exciting vibration force function, which includes static loads as well as the dynamic loads obtained from the superposition of a series of sin functions. In this article, an exciting–vibration force which is corresponding to high, intermediate and low frequency is set to simulate the wheel-rail interactional force, which is namely train load and has irregular responses, additional dynamic loads and wear effect of rail surface. The dynamic load is simplified to the formula as below in reference [11]:

$$F(t) = P_0 + P_1 \sin(\omega t) \qquad (1)$$

Wherein: P_0 means the static load of a single wheel; P_1 is on behalf of corresponding vibrating load, $P_1=M_0a\omega^2$ in which M_0 stands for unsprung weight with a as the vector height and ω as the circular frequency; The passenger train whose axle load is 18T owns M_0=750kg and a=0.7mm。

2.3 Viscoelastic Artificial Boundaries

Generally speaking, when finite-element numerical method is used to solve the problem of soil-structure dynamic interaction, finite-size calculation area needs to be cut out from infinite medium, in the boundaries of which artificial boundaries are put to accomplish the simulation of infinite foundation [12].

By adopting consistent viscoelastic artificial boundaries, it is equivalent to continuously distributed springs (in parallel)-damper system [13], on which spring stiffness and damping coefficients of normal and tangential directions are calculated according to the formula（2）and formula（3）. The unit referring to spring stiffness of normal and tangential directions is kPa/m, whose value is multiplied by the corresponding pressure-sharing area of finite-element model to get the spring coefficient of spring element; The unit of damping in normal and tangential directions is $N\cdot s/m^3$, whose value is multiplied by the corresponding pressure-sharing area of finite-element model to obtain damping coefficient of the spring element.

$$K_{BN} = \alpha_N \frac{G}{R}, \quad C_{BN} = \rho c_p \qquad (2)$$

$$K_{BT} = \alpha_T \frac{G}{R}, \quad C_{BT} = \rho c_s \qquad (3)$$

Wherein: K_{BN} and K_{BT} respectively stand for spring stiffness of normal and tangential directions; C_{BN} and C_{BT} respectively mean damping coefficients of the dampers in the normal and tangential directions; R is the distance from wave source to the artificial boundary point; c_p and c_s respectively stand for the wave velocity concerning wave P and wave S of the medium; G is the shear modulus of the medium; ρ is the mass density of the medium; N and T respectively mean the viscoelastic artificial boundary correction coefficients in the normal and tangential directions and the recommended coefficients are 4/3 and 2/3.

2.4 Model Parameters

Referring to the ballastless track structure of Suining-Chongqing Railway, the length of ordinary A-type concrete track slab is 4.93 m and its width is 2.4 m while the width of CA mortar layer is 2.4 m and the width of the base made of C40 concrete is 3.2 m; the length of spring-damping element is 1cm with spring (stiffness) coefficient being 65 kN/mm and damping coefficient being 50 $kN/m\cdot s^{-1}$. Sine wave form is applied to the train load of 18T axle load: F(t)＝-90000-13250×sinωt,ω=2πf, f=8Hz。Calculating parameters of materials in various structural layers are shown as the Table 1 and finite-element calculation model is shown as the Figure 2, in which the longitudinal length of the subgrade is 10 cm and the lateral length of the foundation is 33 m.

Table 1: *Calculation parameters of system structure layers*

Structure Name	Thickness (*m*)	Modulus of Elasticity (*MPa*)	Natural Volume Weight (kN/m^3)	Poisson's ratio	Internal friction angle (°)	Cohesive force (*kPa*)	Shear Modulus (*MPa*)	c_s (*m/s*)	c_p (*m/s*)
Steel Rail	0.35	206000	78	0.3					
Track Slab	0.19	35000	26	0.17					
CA Mortar	0.05	200	18	0.25					
Concrete Base	0.3	25000	25	0.2					
Surface layer of Roadbed of Graded	0.7	160	22.5	0.3	40	3	60	600	1200

Macadam									
Bottom layer of roadbed of the padding in team A&B	2.3	120	20.5	0.3	36	5	45	500	1000
Subgrade Body of red bed's Mudstone	3.0	80	20	0.3	36	54	30	450	900
Original-state subgrade of red-bed mudstone	6.0	80	19	0.3	42	54	30	2000	4000

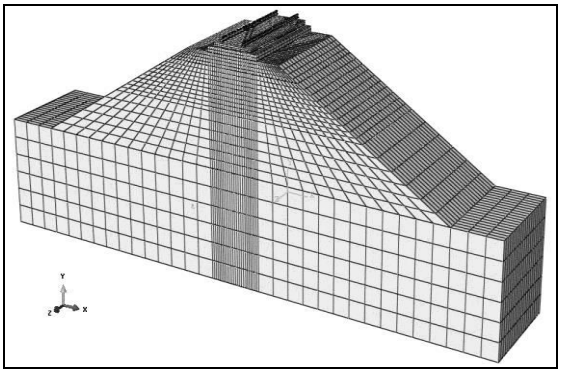

Figure 2: *The finite element model of ballastless track-subgrade system in Sui-Yu railway*

3. Analysis of Calculating Results

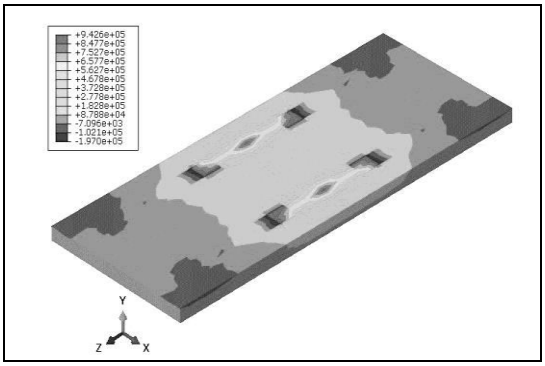

Figure 3: *Stress contours of track plate*

Figure 3 is the stress-distribution diagram of track slab, from which it can be seen that there exist pressing stress and pulling stress simultaneously. And the maximum pressing stress is 943 kPa and the maximum pulling stress is 197 kPa, both of which are far less than their extreme pressure-proof and pulling-proof intensity.

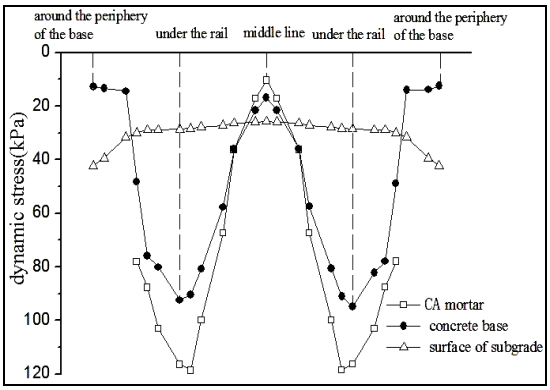

Figure 4: *Lateral distribution of dynamic stress*

Figure 4 is the lateral distribution situation of dynamic stress along the track. Along the direction of track's transverse section, dynamic stress distribution of CA mortar and the base is extremely asymmetrical, the maximum values exist under the rail, and the value of dynamic stress in the position of middle line is the minimum; the dynamic stress distribution on the surface of the subgrade is relatively asymmetrical and the maximum values happen around the base's periphery; But concerning the ballast track structure, dynamic stress is distributed in the shape of a saddle with the maximum values existing under the rail, which is the reason why ballastless track owns better dispersive effect on loads than ballast track does.

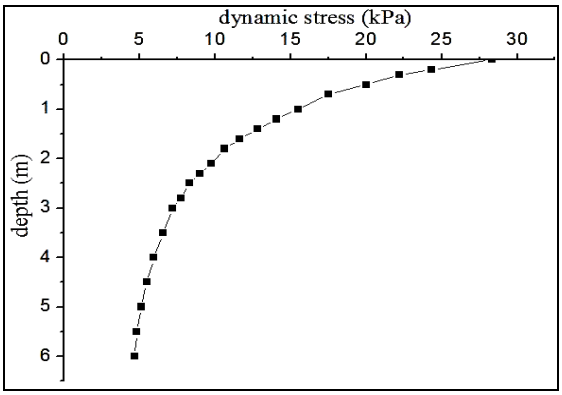

Figure 5: *Distribution of dynamic stress in the depth direction*

Figure 5 is the distribution situation of dynamic stress along the depths of the subgrade. Due to the damping and diffusion function of soil mass, dynamic stress reduces gradually along the depths of subgrade, and referring to the depth of the surface layer of the roadbed, the decay rate is comparatively faster while it is relatively slow in bottom layer of the roadbed; after passing through the surface layer of roadbed, the dynamic stress is reduced by 38% and then after going through the bottom layer of the roadbed, it decays by 75% with roadbed part of the subgrade bear the most part of the stress' effects. In reference [14], the actual measurement is done for the roadbed dynamic stress in the Wuhan-Guangdong passenger special line and it is found that the decay rate of dynamic stress on the subface regarding the surface layer of roadbed is 41% while the decay rate of the subface concerning the bottom surface of the roadbed is 82%, which are basically consistent with the laws obtained from field measurement so that the reliability of model calculation is proved in a further way.

3. Impacts of the train speed

To study the impacts of train running speed on track stress function, there are various influencing factors should be considered and to simplify the complexity of calculation, only the changes of train velocity are taken into account. The running speeds chosen are respectively V=0km/h, 120km/h, 200km/h, 250km/h, 300km/h, 350km/h and 400km/h. The stress responses of the track at different running speeds are analyzed without changing the parameters of various structures in the track.

In the model, the dynamic loads are added to fixed points and the changes of velocities are shown through the variations of loading frequency, so before the different-speed calculation is conducted, it is necessary to figure out the relationship between frequency and speed first. By referring to bogie's wheelbase and the vehicle length of CRH series, the model is shown as Figure 6.

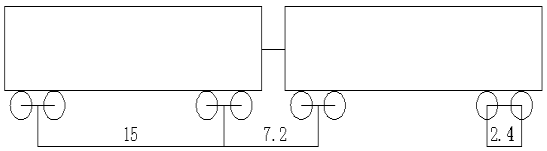

Figure 6: *Carriage structure of CRH train (m)*

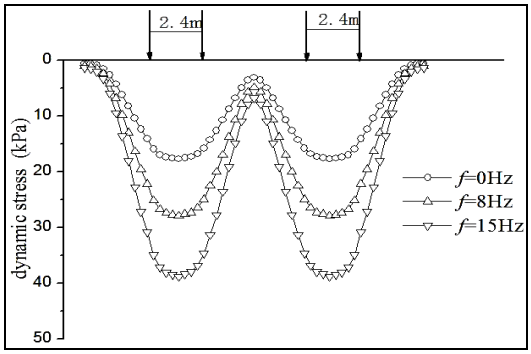

Figure 7: *Vertical distribution of dynamic stress along the line*

Figure 7 is about the longitudinal distribution form of dynamic stress along the roadbed under the effects of two bogies (4 wheel load) between adjacent carriages. It can be seen that under the effects of different loading frequencies, one bogie will produce one dynamic stress wave crest. The most adverse factor should be considered and the distance between the two adjacent wave crests is the distance between two bogies of the adjacent carriages, namely 7.2 m. The transformational relationship between frequency and velocity concluded is as shown in Table 2.

Table 2: *Conversion between frequency and speed*

Velocity (km/h)	0	120	200	250	300	350	400
Frequency (Hz)	0	4.63	7.72	9.65	11.57	13.50	15.43

The influence of train running speed on subgrade's dynamic function is analyzed by means of trains' axle weight 18T and the superposition of dynamic stress is taken into account. Results of all calculations of working conditions below are acquired under the effect of one bogie (two wheel loads).

3.1 Impacts of Train Speed on Track Structure

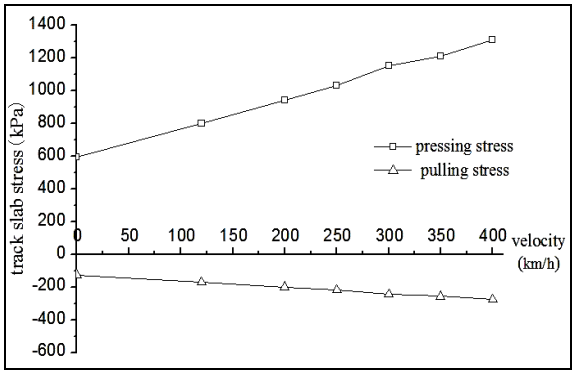

Figure 8: *The influence of speed on track plate stress*

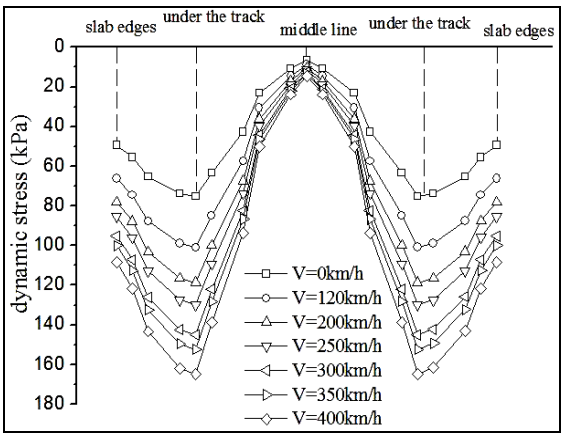

(a) Bilateral distribution of dynamic stress

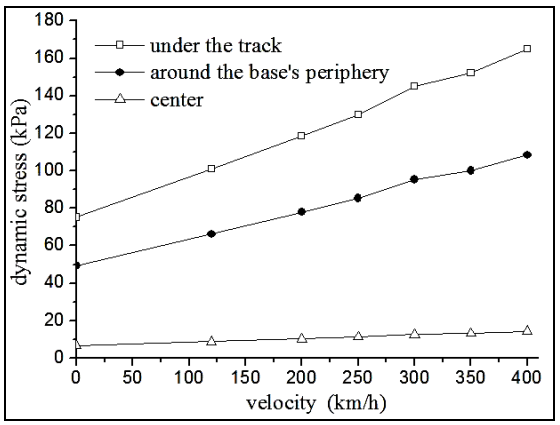

(b) The relationship between dynamic stress and velocity

Figure 9*: The influence of speed on the dynamic stress of CA mortal layer*

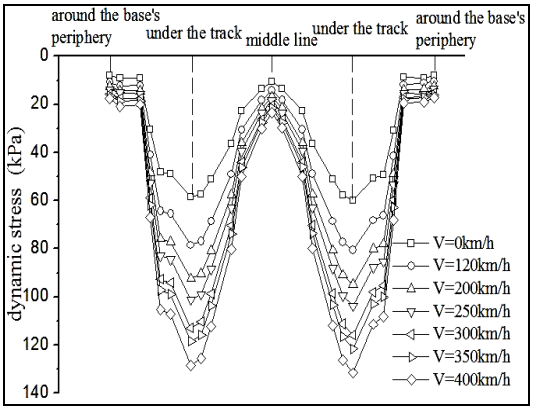

（a）The lateral distribution of dynamic stress

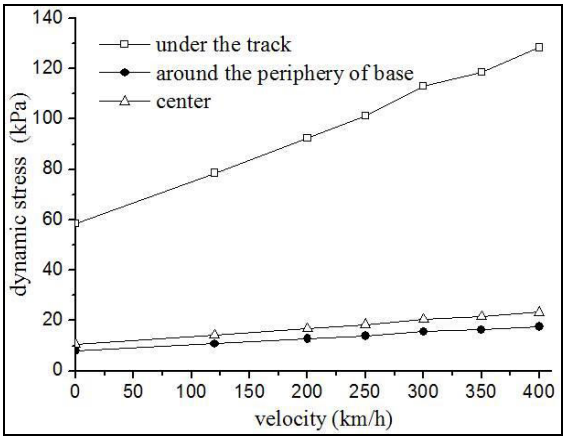

（b）The relationship between dynamic stress and train running speed

Figure 10: *The influence of speed on the dynamic stress of concrete base*

Figure 8 shows the impacts of train's running speed on track slab stress. The maximum pressing stress and pulling stress of the track slab basically have a linear increasing relationship with the running speed. Meanwhile, the pressing stress increases relatively quicker.

Figure 9 is about the impacts of the trains' running speed on the dynamic stress of CA mortar layer. It can be seen from the figure that the speed has bigger influence on dynamic stress under the track and around the peripheries while comparatively less influence on dynamic in the middle-line position. When the velocity increases from 5 km/h to 400 km/h, the dynamic stress under the track increases from 75,269kPa to 164.844kPa with an increase of 120%; the increasing ranges under the track, on the edges of the slab and in the middle line varies, but all of them have a linear increasing relationship with the velocity. Figure 10 refers to effects of train running speed on concrete bases, from which it can been seen that there is a linear increasing relationship between dynamic stress and velocity in different positions of the base. The influence of velocity towards the dynamic stress under the track is very big while the impacts of speed on dynamic stress around the peripheries and in the middle line are less.

3.2 The Influence of Train's Speed on Subgrade Structure

Figure 11 is about the effects of train's running speed on dynamic stress concerning the surface of subgrade, from which it can be figured out that within the range of the base, dynamic stress rises with the increasing train velocity. The maximum value of dynamic stress occurs near the edges of the base, balanced distributed dynamic stress with the range of the base and the subgrade surface outside the base is not affected by the stress. The increasing ranges of dynamic stress under the track, at the edges of the base and in the middle line varies, but all of them have a linear increasing relationship with the velocity, which rises from 5km/h to 400km/h and corresponding dynamic stress increases from 17.95kPa to 39.365kPa with an increase of 120% or so.

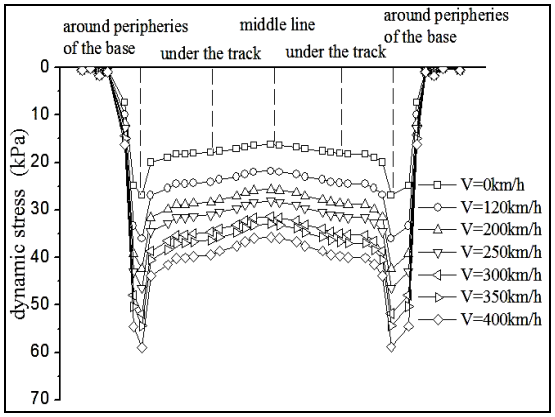

（a）Bilateral distribution of dynamic stress

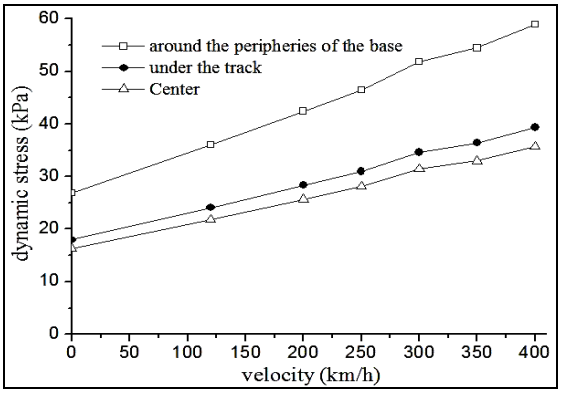

(b) The relationship between dynamic stress and train's running speed

Figure 11: *The influence of speed on the dynamic stress of subgrade surface*

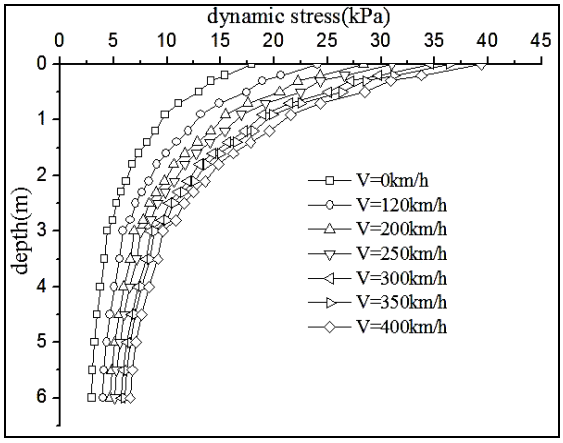

（a）Depth distribution along the subgrade

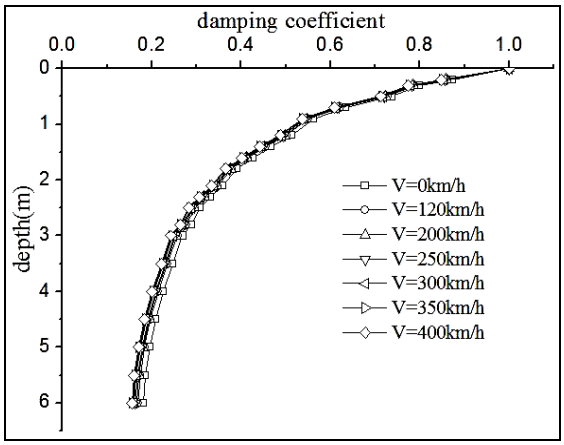

（b）Damping of depth along the subgrade

***Figure 12:** The influence of speed on the distribution of dynamic stress along subgrade depth*

Figure 12 (a) shows the attenuation coefficient of dynamic stress along the subgrade. With the increase of train's speed, the dynamic stress of different depths in subgrade all grows and the adding value on the surface of the subgrade is the largest. The deeper the depth is, the smaller adding value will be.

The normalization is conducted to the dynamic stress, that is, handle test data of every team based on $\sigma_{di}/\sigma_{dmax}$, of which σ_{dmax} is the dynamic stress value of the subgrade surface. The damping law of stress based on the depths along the subgrade is shown as Figure 12 (b), which means that the damping law of dynamic stress under various speeds varies within a very small range, namely very little impacts of speeds on stress. The dynamic stress decreases by 38% within range of surface layer in subgrade (0.7 m depth) while stress decreases by 75% on the bottom layer of subgrade (3m depth).

4 Conclusions

(1)The maximum pressing stress and pulling stress value of the track slab is far less than its ultimate pressure-proof and tensile-proof intensities; In the lateral direction along the track, the maximum dynamic stress of CA mortar and the base exist under the track while the dynamic stress of the subgrade's surface is distributed evenly with the maximum value occurring around the peripheries of the base; dynamic stress gradually decreases with the depths of the subgrade and the damping rate of dynamic stress on the surface layer of roadbed is quicker than that in the bottom layer of the roadbed.

(2)One bogie of the train produces one dynamic stress wave crest, and in the finite-element simulating calculation, the most adverse factors should be considered. Moreover, to obtain the transformational relationship between frequency and velocity, the distance between two bogies of adjacent carriages, namely the distance between two adjacent wave peaks, should be acquired.

(3)There is a linear increasing relationship between the dynamic stress of track slabs, CA mortar, the base and foundation and the velocity, but dynamic stress of different positions owns various increasing ranges; Along the depth of the subgrade, with the growth of running speed, the stress on the surface owns the largest adding value while with the increase of the subgrade depth, the adding value decreases gradually; After the normalization of dynamic stress, it is found that train's velocity has little influence on the damping rate of stress with the rise of depth.

Acknowledgement:

This work was supported by the Scientific and Technological Development Plan of Ministry of Railways under NO. 2010G003-F.

References:

[1] SONG X L, ZHAI W M. China Railway Science, 33 (2012) 1.
[2] LEI X Y, ZHANG B, LIU Q J. Journal of Vibration and Shock, 29 2010 168.
[3] KONG X H, JIANG G L, WANG Z M. Hydrogeology & Engineering Geology, 39 (2012) 75.
[4] JIANG G L, KONG X H, MENG L J, et al. Journal of Southwest Jiaotong University, 45 (2010) 855.
[5] GUO Z G, WEI L M, ZHOU Z Y, et al. Hydrogeology & Engineering Geology, 40 (2013) 51.
[6] Pedro A C, Rui C, Antonio S C, et al. Soil Dynamics and Earthquake Engineering, 30 (2010) 221.
[7] G. Lombaert, G. Degrande, J. Kogut, S. Franc - ois, Journal of Sound and Vibration, 297 (2006) 512.
[8] Sheng X, Jones CJC, Thompson DJ. J Sound Vib, 293 (2006) 575.
[9] Hall Lars. Soil Dynamics and Earthquake Engineering, 23 (2003) 403.
[10] LIANG B, CAI Y. Journal of the China Railway Society, 21 (1999) 84.
[11] KONG X H, JIANG G L, LI A H, et al. Journal

of Southwest Jiaotong University, 49 (2014) 406.
[12] LI J S, LI K C. Journal of the China Railway Society, 17 (1995) 66.
[13] DONG L, ZHAO C G, CAI D G, et al. China Civil Engineering Journal, 41 (2008) 81.
[14] ZHOU Z Y. Changsha: Central South University, 2010, p.47.